[1.]Khalid Ali KHAN, [2.]Mukesh PATHELA

IMPACT OF BREWSTER PLATE THICHNESS ON ISOMETRIC STRUCTURE OF W- SHAPED OPTICAL CAVITY

[1.]Department of Electrical and Computer Engineering, Mettu University, Mettu, PO. Box-318, ETHIOPIA.
[2.]Department of Electronics & Communication Engineering, DBIT, Dehradun, INDIA

Abstract: Optical cavities having different shapes and architecture offer distinguished platform for research and investigation. In this paper, W shaped optical cavity is designed with the help of two flat mirrors, three spherical mirrors and a Brewster crystal plate. The impact of Brewster crystal plate thickness and its refractive index variation on the state of stability and beam profile are analyzed through simulation. Suggested models reflect the same results for all investigating parameters but the difference in crystal positioning shifts its effect according to its respective location. The total cavity length of 904.88 mm is matched with pulse repetition rate of 165.652MHz or inter-mode frequency to cover the round-trip distance of 1811.025 mm in the cavity. The minimum beam waist is found in the sagittal plane at the reflecting surface of the third spherical mirror.
Keywords: W- shaped cavity, ABCD matrix, Brewster crystal plate, Beam radius, Stability

1. INTRODUCTION

Novel optical cavity or resonator is the important component in modern optical amplifier. its wide, advance, and large variety of scientific applications, including photonic integrated circuits are the next generation in optical components. Laser and associated cavity are the new research trend in optical fiber communication, light detection and ranging, optical coherence tomography (OCT) and high- resolution laser spectroscopy [1].Larger path- length-cavity is required to enhance the sensitivity of laser spectroscopy as it meets the larger interaction between intracavity radiation and absorbing sample [2].Different structure of cavities according to its application has been the matter of interest [3-5] from beginning, nevertheless there is a continual development in its novel version. Analysis of the cavity is carried out in several ways or in terms of the cavity fitness and its measurement [6-7], Q-factor, and stability [8], alignment of the cavity [9], nanotube microcavities [10], optomechanical cavities [11] and many more.

Physical thickness (ℓ) and refractive index(n) is the characteristics of Brewster crystal plate.it is widely used as a laser gain medium. When laser rod experience too shorter in length, in this case Brewster crystal is treated as plane parallel-plate tilted at Brewster angle (Θ) toward beam propagation. So, a tilted crystal plate always establishes the longer geometric path(L_{eff}) for the beam. Here, it can be fairly seen in figure 1 that, $L_{eff} > \ell$. Refractive index, physical thickness and L_{eff} is related as equation 1.A simple Brewster crystal plate can be seen in "Figure 1".

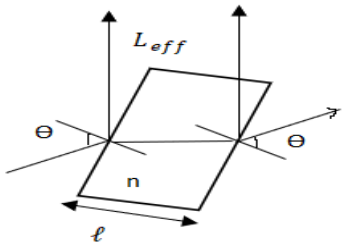

Figure 1: Brewster Crystal plate

$$L_{eff} = \frac{\ell}{\cos\left(\arcsin\left(\frac{\sin(\arctan(n))}{n}\right)\right)} = \frac{\ell\sqrt{n^2+1}}{n} \quad (1)$$

Table 1: ABCD Matrix for optical component

Optical Component	ABCD Matrix	Description
Empty Length	$M_T = M_S = M = \begin{bmatrix} 1 & L \\ 0 & 1 \end{bmatrix}$	L=Empty length M_T=ABCD matrix in T plane M_S=ABCD matrix in S plane
Flat Mirror	$M_T = M_S = M = \begin{bmatrix} 1 & 0 \\ 0 & 1 \end{bmatrix}$	It has unit matrix and does not affect beam propagation
Spherical Mirror	$M_T = \begin{bmatrix} 1 & 0 \\ -\frac{2}{R.\cos\alpha} & 1 \end{bmatrix}; M_S = \begin{bmatrix} 1 & 0 \\ -\frac{2.\cos\alpha}{R} & 1 \end{bmatrix}$	R=Radius of curvature α =Beam incidence angle
Brewster Crystal Plate	$M_T = \begin{bmatrix} 1 & \frac{\ell.\sqrt{n^2+1}}{n^4} \\ 0 & 1 \end{bmatrix}; M_S = \begin{bmatrix} 1 & \frac{\ell.\sqrt{n^2+1}}{n^2} \\ 0 & 1 \end{bmatrix}$	ℓ=thickness of crystal n=refractive index of crystal

In this paper, a simple W- shaped cavity in order to increase the path length for intracavity radiation is demonstrated and simulated. Influence of the Brewster crystal plate at the respective arm and its position, impact of crystal thickness(ℓ) and its refractive index(n) on the beam profile in tangential (T) and sagittal (S) plane has been also tested. The beam radius variation before the crystal plate, inside the crystal and after the

crystal plate is also computed graphically. Additional effort to compare the performance in the respective plane of observation (T and S) for the both models suggest new potential mechanism for stable cavity and Gaussian beam generation in standing-wave (SW) system. Ray transmission characteristic of every element is represented by conventional ray matrix (ABCD matrix). Derived ABCD matrix for empty space, flat mirror, spherical mirror, and Brewster crystal plate is tabulated in "Table 1" [11-12]. During simulation, Normal stability parameter($\frac{A+D}{2}$) is used to check the system stability, wherein its values lie in between -1 to +1.

2. MODELLING AND ITS RAY TRANSFER MATRIX (ABCD MATRIX)

Simple and most efficient W -shaped optical cavity with compensating crystal (Cr) plate can be modeled as proposed configurations, which are shown in "Figure 2 (a)" and "Figure 2 (b)". Both models are developed by two flat mirrors (M1, M4), three spherical mirrors (M2, M3, M4). An astigmatically compensated-crystal-plate (thickness =1mm, refractive index=1.6) is also inserted in between spherical mirror of an intermediate arm. Here, the distance between M4 and M5, M1 and M2 is referred as the first folding range(L2) and second folding range (L1) respectively. Inclination angle (α) resemble the folding angle for mirrors and suitably matched with optical beam incidence angle. Curvature of cavity mirrors, beam incidence angle, operating wavelength (1000 nano meter) are the controlling parameters in order to meet the stability of the cavity for standing-wave (SW) system. These models are almost similar except their Cr positioning to its respective arms. Compensating crystal (Cr) is fixed in the second arm for model-1 and in fourth arm for model-2. Lc2 represents the distance of the crystal from mirror M3 in both models, whereas Lc1 shows the crystal position from M2 and M4 in model-1 and model-2 respectively. The adjusted and specific values of all components are compiled in "Table 2" with its ABCD matrix.

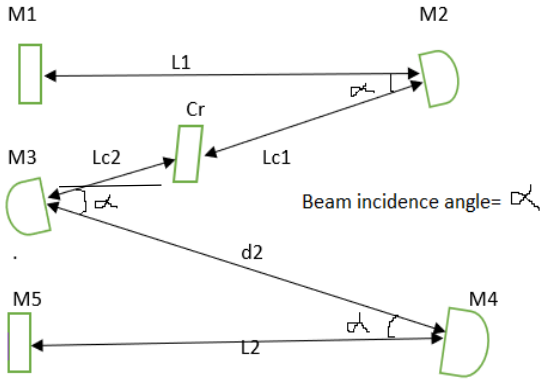

Figure 2(a): W-Shaped cavity model-1

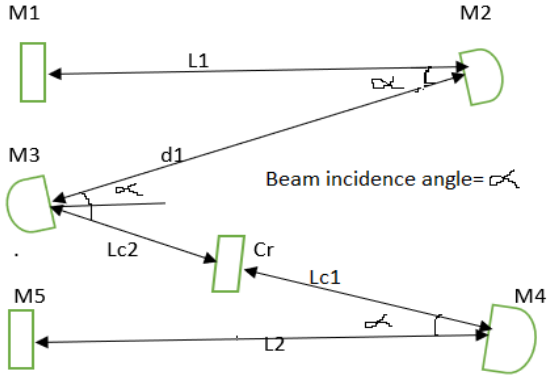

Figure 2(a): W-Shaped cavity model-2

Table 2: ABCD Matrix of optical component as per designed specification

Optical Component	ABCD Matrix	Description
Flat Mirror (M1, M5)	$M_T = M_S = \begin{bmatrix} 1 & 0 \\ 0 & 1 \end{bmatrix}$	M_T=Matrix in Tangential Plane M_S= Matrix in Sagittal plane
Free Space (L1, L2)	$M_T = M_S = \begin{bmatrix} 1 & 400 \\ 0 & 1 \end{bmatrix}$	Length L1=Length L2=400mm
Empty Space Lc1	$M_T = M_S = \begin{bmatrix} 1 & 25 \\ 0 & 1 \end{bmatrix}$	Length Lc1=25 mm
Empty Space Lc2	$M_T = M_S = \begin{bmatrix} 1 & 26 \\ 0 & 1 \end{bmatrix}$	Length Lc2=26 mm
Empty Space d1, d2	$M_T = M_S = \begin{bmatrix} 1 & 52 \\ 0 & 1 \end{bmatrix}$	Length d1=length d2=52mm
Spherical Mirror (M2, M4)	$M_T = M_S = \begin{bmatrix} 1 & 0 \\ -0.02 & 1 \end{bmatrix}$	Radius of curvature=100 mm Inclination in M2, M4=7^0
Spherical Mirror (M3)	$M_T = M_S = \begin{bmatrix} 1 & 0 \\ -0.04 & 1 \end{bmatrix}$	Radius of curvature =50 mm Inclination in M3=7^0
Brewster Crystal Plate (Cr)	$M_T = \begin{bmatrix} 1 & 0.288 \\ 0 & 1 \end{bmatrix}$, $M_S = \begin{bmatrix} 1 & 0.737 \\ 0 & 1 \end{bmatrix}$	Brewster plate thickness(ℓ)=1mm Refractive index (n)=1.6 Inclination in Crystal plat =7^0

Overall round-trip matrix (M0) for both models by considering M5 (output element) as a reference element, can be calculated with the help of equation 2 and equation 3. Thus,

$$M0_{model\ 1} = M5 * L2 * M4 * d2 * M3 * Lc2 * Cr * Lc1 * M2 * L1 * M1 * L1 * M2 * Lc1 * Cr * Lc2 * M3 * d2 * M4 * L2 \quad (2)$$

$$M0_{model\ 2} = M5 * L2 * M4 * Lc1 * Cr * Lc2 * M3 * d1 * M2 * L1 * M1 * L1 * M2 * d1 * M3 * Lc2 * Cr * Lc1 * M4 * L2 \quad (3)$$

3. SIMULATED RESULT AND DISCUSSION

— Stability parameter and Brewster crystal parameters

As it is explained in previous section, W-shaped folded cavity has two models in which first one hold Brewster plate in second arm (in between M2 and M3) whereas in second model, Brewster plate is placed in third arm (in between M3 and M4). In both model, stability of the cavity is unaffected by the variation of refractive index (n) of Brewster crystal. "Figure 3" reveals that simulated stability parameter lies in the range of -0.9 to -0.3, for minimum refractive index to maximum of 2.5 in both plane of observation. Of course, this stability values are in between -1 to +1 which is a satisfactory condition for laser operation. Refractive index (n) versus stability($\frac{A+D}{2}$) variation plots are similar same for both model in S and T plane simultaneously under the same boundary condition. But, a serious impact of crystal thickness variation may be observed on the state of cavity stability, wherein wider thickness of crystal (ℓ > 15 mm) disturb the stability in S plane for both models. But, Stability in tangential plane (T) remains unaffected and its explanation can be understood by "Figure 4 (a)", and "Figure 4(b)" for both models respectively. Expression (4) and (5) ensures the crystal thickness confinement under respective stability boundaries as,

$$-1 \leq \frac{A+D}{2} \leq +1 \text{ exist, either if } \ell \leq 5\text{mm or } 7\text{mm} \leq \ell < 15, \text{in S plane} \quad (4)$$

$$-1 \leq \frac{A+D}{2} \leq 0 \text{ exist, either if } \ell \leq 9\text{mm or } 11\text{mm} \leq \ell \leq 25, \text{in T plane} \quad (5)$$

But, in contrast to expression (4) and (5), if crystal thickness lies in between 5 mm to 7 mm, or in between 9 mm to 11mm then stability is violated in S and T plane respectively.

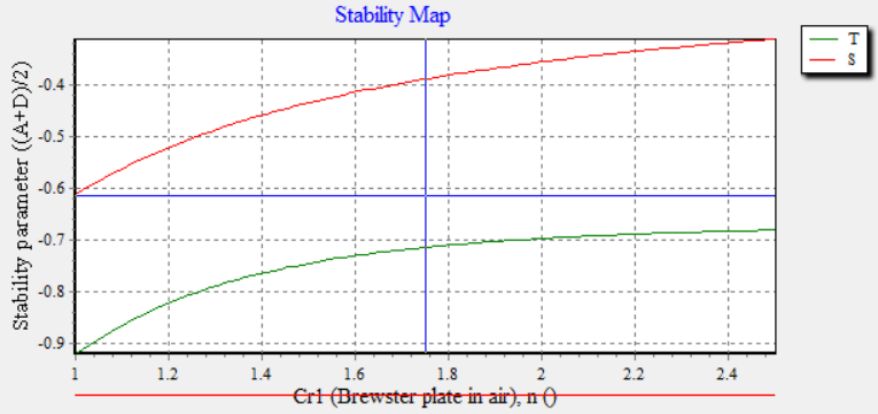

Figure 3: Refractive Index verses Stability Variation graph for both models

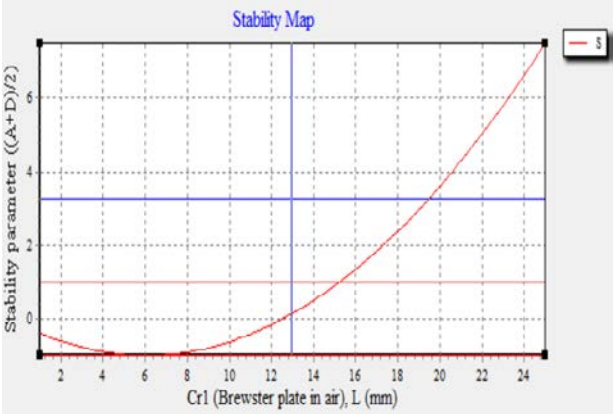

Figure 4(a): Stability versus crystal width in S plane

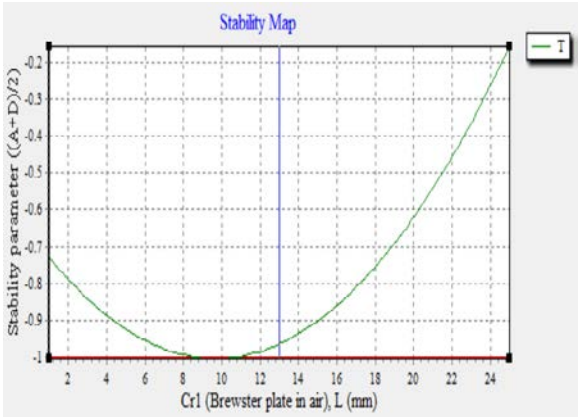

Figure 4(b): Stability versus crystal width in T plane

"Figure 4(a, b)" strongly demonstrate that stability adjustment is a more sensitive task for both models in the S plane because, its values lie in between -1 to +1 only if the crystal width is adjusted carefully otherwise stability will be lost. Whereas, stability does not disturb in the T plane for the same case, because the entire value of the stability parameter is found in the range of -1 to -0.2 which satisfies its boundary condition. Parabolic curve reveals that at two different crystal thickness, there will be a same state of stability. Parabolic curve has been recorded for the following thickness that is $0<\ell<10$ mm and $0<\ell<18$ mm in S and T plane respectively. It can be also explained more clearly as, if stability parameter ($\frac{A+D}{2}$) is reaches to lower than -0.65, crystal plate commences its two distinct thickness inherently in S plane. At the same time, dual values of crystal thickness can be also seen in T plane, when the same stability parameter comes under the limit of -

$0.74 < \frac{A+D}{2} < 1$.Minor stability variation(from-0.1 to -1.0) in T plane because of large thickness variation (from 1 mm to 25 mm) of crystal plate recognize the authentication of beam profile in this plane. So, a thin Brewster crystal plate ($\ell \leq 5mm$) is always suitable to get the stable laser operation in both plane of observation.

— Beam Radius Variation in a Crystal and in a Cavity

In this section, the variation in beam radius is investigated and reported along the first folding range, inside the crystal and along the entire cavity. A point in the first folding range that is at a distance of 300mm from the M4 is chosen to record the observation. " Figure-5(a, b)" claims that with increase of crystal-thickness, beam radius decreases in both plane (S,T) .It may be more interesting to note that , dual curve profile of beam radius variation are also traced in both plane of observation which are the consequences of existence of two different crystal- thicknesses for same state of stability. A separation between dual curves allocate the crystal thickness range over which a single thickness value is responsible for a single state of stability. For example, a separation from 5.14 mm to 7.01 mm in crystal thickness as depicted in "Figure 5(a)" in S plane region predicts the range of single crystal thickness that offer the single state of stability and similar philosophy may be applied for "Figure 6(b)". However, wider crystal variation is required in T plane for the same beam radius variation as found in S plane because right shifting of green twin curves (in S plane) in comparison to red twin curves (in S plane) is more flattened and extended along x-axis. Beam radius plot along second arm (Figure-6(a)) indicates beam size reduction while traveling from M2 to M3 in both planes. Furthermore, a peculiar phenomenon happens at the surface of the crystal plate, at which the beam radius is abruptly increased by 161 mm (430.9 mm-269.3 mm) only in S plane. This magnification can be measured in between 25mm to 26 mm from mirror M2 in second arm and exactly at Cr position. But an insignificant beam magnification is recorded in the case of T plan. "Figure 6(b)" also justify the same phenomenon in the third arm for model-2 at which Cr is placed. Therefore, "Figure 6(b)" is a replica of "Figure 6(a)" in order to study the beam profile along the arm that hold the crystal.

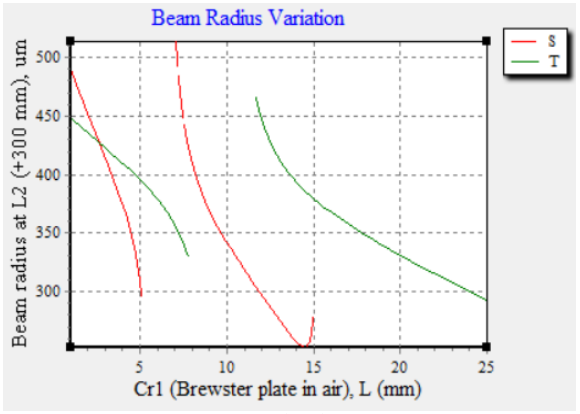

Figure 5(a): outward shift of "L verses beam radius "in T plan at L2==300 mm, ℓ=1 mm, n=1.6 for model-1

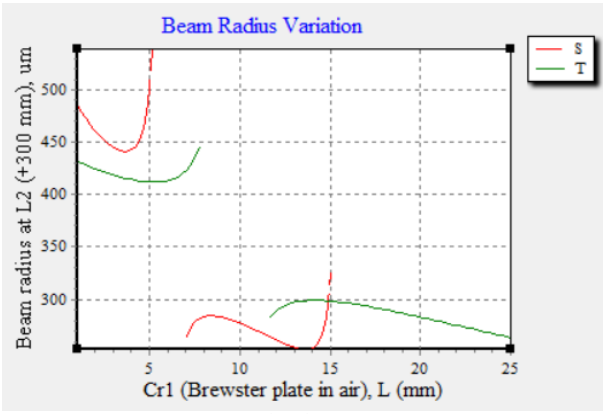

Figure 5(b): outward shift of "L" verses beam radius in T plan at L2==300 mm, ℓ=1 mm, n=1.6 for model-2

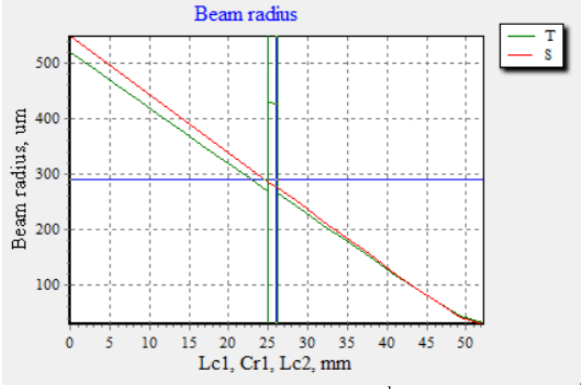

Figure 6(a): Beam radius along 2nd arm in model-1

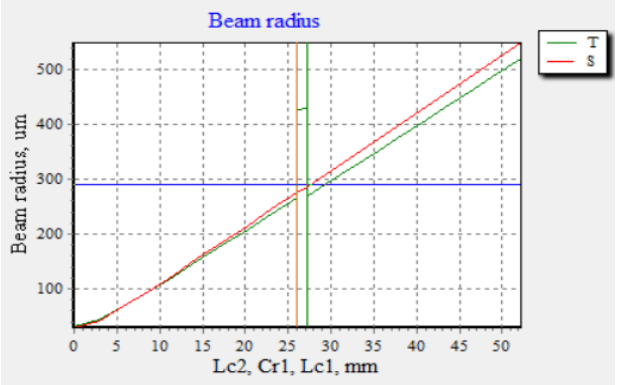

Figure6(b): Beam radius along 3rd arm, at ℓ=1mm in model-2

Additional "Figure 6(c)" and "Figure 6(d)" shows the beam radius amplification at the crystal position with crystal thickness(ℓ) of 5 mm and at 10 mm respectively.it can be noticeably recorded that at ℓ=10 mm, laser operation by the cavity is stopped in the tangential plane. Thus, beam variation plot can be only visualized in sagittal plane that is depicted in "Figure 6(d)". The beam shapes along the individual arm changes from one point another point and it depends upon the difference in beam radius that are found in sagittal as well as in tangential plane. If difference is zero, shape will be circular otherwise elliptical.

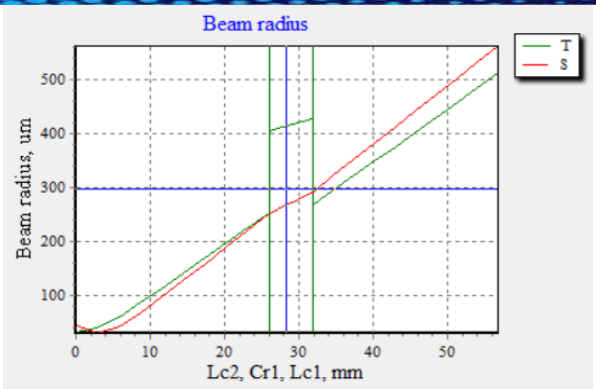

Figure 6(c): Beam radius along 3rd arm, at ℓ=5mm in model-2

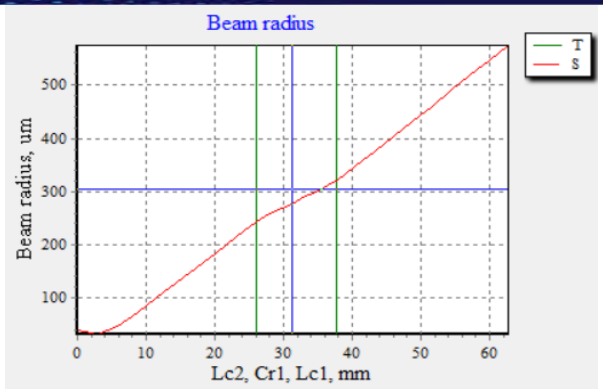

Figure 6(d): Beam radius along 3rd arm, at ℓ=10mm in model-2(Unstable in T plane)

It can be clearly explained by "Figure 6 (c)" that at ℓ=5mm, maximum difference in beam radius to its respective plane is recorded on the right edge of the crystal facet. Hence,

$$\text{Beam radius in tangential plane} = |w_t|_{\text{at 31mm from M3}} = 426.47 \text{ mm} \quad (6)$$

$$\text{Beam radius in sagittal plane} = |w_S|_{\text{at 31mm from M3}} = 289.97 \text{ mm} \quad (7)$$

So, Larger difference in beam radius (difference in w_t and w_S) as obtained in (6) and (7) yields larger elliptical beam irrespective of arms. Whereas smaller difference in beam radius in respective plane diminished ellipticity from the shape and comes closer to circular shape as found in by (8) and (9). Different beam shapes, beam radius in respective plane and its $\frac{w_t}{w_S}$ ratios are collectively presented in figure 7.

$$\text{Beam radius in tangential plane} = |w_t|_{\text{at 25.8 mm from M3}} = 251.77 \text{ mm} \quad (8)$$

$$\text{Beam radius in sagittal plane} = |w_S|_{\text{at 25.8 mm from M3}} = 249.87 \text{ mm} \quad (9)$$

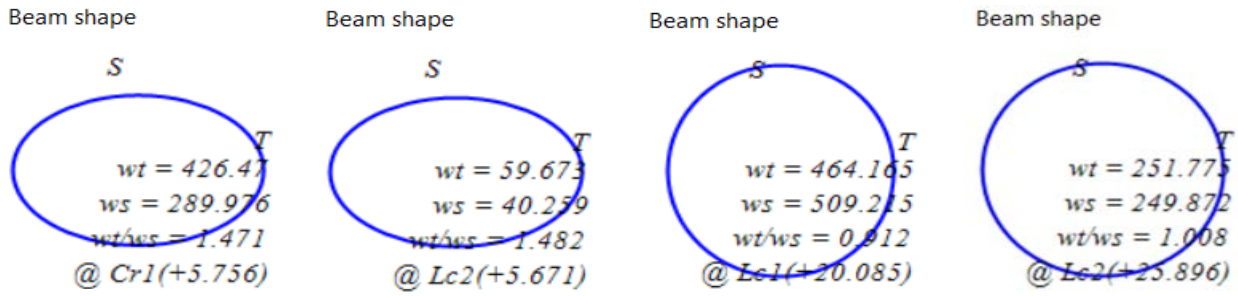

Shape at $w_t \gg w_S$ | Shape at $w_t > w_S$, | Shape at $w_t \ll w_S$ | Shape at $w_t \approx w_S$

Figure 7: Different beam shapes with relative value of w_t and w_S

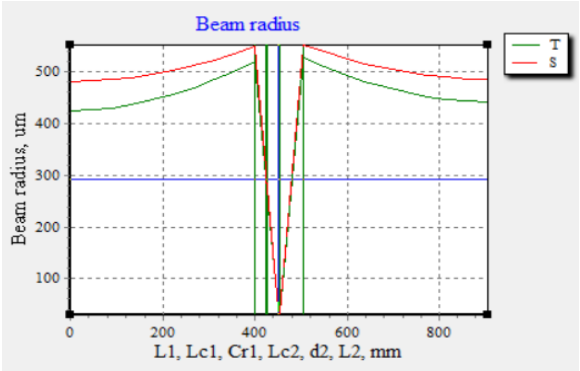

Figure 8(a): Beam radius variation along cavity model-1

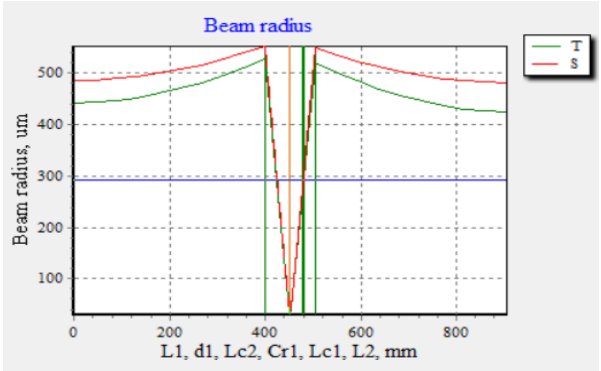

Figure 8(b): Beam radius variation along cavity model-2

Evolution of beam radius in in sagittal(S) and tangential (T) plan is depicted in "Figure-8(a, b)". The beam size on the folding -range arms are larger than other arms and a sudden contraction in beam radius is recorded in between spherical mirrors (in between M2 to M3 to M4, in both models). Eventual and abruptly hike in beam radius at the surface of Cr plate is also appearing in the tangential plane due to refraction of the beam because of the refractive index of the crystal. Sharp fall or rise in beam radius along d1 and d2 depends upon the nature of spherical mirrors and its folding angles. Beam that comes closer to M3 appears as a smaller beam spot. Here both models furnish the smallest beam spot of 30 um radii in S plane, which is found at the position of 452mm in the cavity from M1. Beam radius variation along intermediate arms (d1, d2) has been also included in "Figure 8 (a)" and "Figure 8(b)" for model-1 and model -2 respectively.

Round-trip matrix (Mo) can be obtained by using equation (2), equation (3) and respective elemental ABCD matrix from "Table-2" for both models in the tangential and sagittal plane as.

$$M_T = \begin{bmatrix} -0.73 & 420.015 \\ -0.001 & -0.73 \end{bmatrix}, \quad M_S = \begin{bmatrix} -0.414 & 676.691 \\ -0.001 & -0.414 \end{bmatrix} \quad \text{Round trip matrix for Model 1}$$

$$M_T = \begin{bmatrix} -0.73 & 338.452 \\ -0.001 & -0.73 \end{bmatrix}, \quad M_S = \begin{bmatrix} -0.414 & 663.767 \\ -0.001 & -0.414 \end{bmatrix} \quad \text{Round trip matrix for model 2}$$

Cavity length of the designed system is 904.88 mm and it offers the inter-mode-beat frequency of 165.652MHz. The optical pulse repetition rate of 165.652 MHz ensures the round-trip distance of 1811.025 mm inside the cavity. A round-trip distance for an oscillating pulse inside the cavity is equivalent to its wavelength(λ) and has to be calculated as equation 10. Therefore,

$$\text{Round} - \text{trip disatnce in a cavity} = \frac{C}{f} \text{ meter} \qquad (10)$$

where, C is the speed of light in vacuum and f is the inter-mode-beat frequency in hertz.

4. CONCLUSION

A precision model for W shaped cavity with Brewster crystal plate is investigated and it is noteworthy that crystal refractive index variation up to a maximum value of 2.5 does not affect the stability of the cavity. Moreover, the crystal thickness variation may alter the stability. Strong thickness stability is observed in T plane cavity. The parabolic curve between stability versus thickness shows a peculiar dual values of crystal thickness that offer the same stability point and it may because of equal beam radius at the point of observation .Presence of crystal plate is the cause of beam radius amplification more precisely in S plane when beam is incident over it, but the amplification reduces with increase of crystal plate thickness if large increment in crystal thickness is deployed beyond a certain limit as laser operation may be lost in that plane. Refer to the "Figure 8(a, b)", it is found that contraction in beam starts after M2 and reaches up to M3 with smallest radius of 31.74 um x 30.01 um in TxS plane. Hereafter, it starts to rise and regain its same value at M4. The beams elliptical in shape and larger in size are generated on both folding range because of larger difference in tangential plane radius and sagittal plane radius of the same beam. However, this beam in the region of contraction looks like a circular (spot) and smaller in size. Proposed cavity may be highly compatible in signal amplification for ultra-short optical pulses (like solitons) in future. The solitons-based transmission technology provides dispersion free transmission in optical fiber communication, which is the integral part of high-speed generation (5G, 6G) technologies.

References

[1] Kevin T. Cook, Pengfei Qiao, Jipeng Qi, Larry A. Coldren, and Connie J. Chang-Hasnain1, "Resonant-anti resonant coupled cavity VCSELs "Vol. 27, No. 3 | 4 Feb 2019.

[2] G. Gagliardi and Hans-Peter Loock "Cavity-Enhanced Spectroscopy and Sensing" the Springer Series in Optical Sciences book series (SSOS, volume 179), Springer-Verlag Berlin Heidelberg, 2014.

[3] IS Amiri, Ahmed Nabih Zaki Rashed," Numerical investigation of V shaped three elements resonator for optical closed loop system", Indonesian Journal of Electrical Engineering and Computer Science Vol. 16, No. 3, pp. 1392-1397, 2019.

[4] Sree Nirmillo Biswash Tushar, Susanta Dev Nath, Jobaida Akhtar, Mohammad Istiaque Reja, "Modelling and Analysis of Z Folded Solid State Laser Cavity with Two Curved Mirrors", International Journal of Microwave and Optical Technology, Vol.13, No.3, pp-244-253 2018.

[5] Iraj S. Amiri, Ahmed Nabih, Zaki Rashed, P. Yupapin," Z Shaped like resonator with crystal in the presence of flat mirror based standing wave ratio for optical antenna systems", Indonesian Journal of Electrical Engineering and Computer Science Vol. 17, No. 3, pp. 1405-1409, 2020,

[6] Gianluca Galzerano, Edoardo Suerra, Dario Giannotti, Francesco Canella, Edoardo Vicentini, and Simone Cialdi, "Accurate Measurement of Optical Resonator Finesse" 9, IEEE Transactions on Instrumentation and Measurement, Jan 2020.

[7] A.B. Mundt A. Kreuter C. Russo C. Becher D. Leibfried∗ J. Eschner F. Schmidt-Kaler R. Blatt," Coherent coupling of a single $^{40}Ca^{+}$ ion to a high-finesse optical cavity", Applied Physics B, Laser and Optics, B-76, pp-117-124, 2003.

[8] H. Kogelnik and T. Li, "Laser Beams and Resonators" Proceedings of the IEEE, Vol. 54, NO. 10, pp-1312-1329, 1966.

[9] Dana Z. Anderson, "Alignment of resonant optical cavities", Applied Optics, Vol. 23, No. 17, pp-2944-2949, 1984.

[10] Yiyang Gong, Armand Rundquist, Arka Majumdar, and Jelena Vuckovi ," Low power resonant optical excitation of an optomechanical cavity", Vol. 19, No. 2 , Optics Express, pp-1429-1440, 2011.

[11] H. Kogelnik, "Imaging of optical mode-Resonators with internal lenses," Bell Sys. Tech. J., vol. 44, pp. 455-494, 1965.

[12] H. Kogelnik, "On the propagation of Gaussian beams of light through lens like media including those with a loss or gain variation," Appl. Opt., vol. 4, pp. 1562-1 569, 1965.